



HAL
open science

Volcanic unrest of the Colli Albani (central Italy) detected by GPS monitoring test

F. Riguzzi, G. Pietrantonio, R. Devoti, S. Atzori, M. Anzidei

► **To cite this version:**

F. Riguzzi, G. Pietrantonio, R. Devoti, S. Atzori, M. Anzidei. Volcanic unrest of the Colli Albani (central Italy) detected by GPS monitoring test. *Physics of the Earth and Planetary Interiors*, 2009, 177 (1-2), pp.79. 10.1016/j.pepi.2009.07.012 . hal-00585472

HAL Id: hal-00585472

<https://hal.science/hal-00585472>

Submitted on 13 Apr 2011

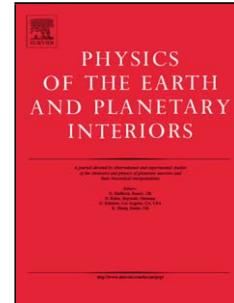
HAL is a multi-disciplinary open access archive for the deposit and dissemination of scientific research documents, whether they are published or not. The documents may come from teaching and research institutions in France or abroad, or from public or private research centers.

L'archive ouverte pluridisciplinaire **HAL**, est destinée au dépôt et à la diffusion de documents scientifiques de niveau recherche, publiés ou non, émanant des établissements d'enseignement et de recherche français ou étrangers, des laboratoires publics ou privés.

Accepted Manuscript

Title: Volcanic unrest of the Colli Albani (central Italy)
detected by GPS monitoring test

Authors: F. Riguzzi, G. Pietrantonio, R. Devoti, S. Atzori, M.
Anzidei



PII: S0031-9201(09)00155-1
DOI: doi:10.1016/j.pepi.2009.07.012
Reference: PEPI 5187

To appear in: *Physics of the Earth and Planetary Interiors*

Received date: 17-2-2009
Revised date: 29-5-2009
Accepted date: 10-7-2009

Please cite this article as: Riguzzi, F., Pietrantonio, G., Devoti, R., Atzori, S., Anzidei, M., Volcanic unrest of the Colli Albani (central Italy) detected by GPS monitoring test, *Physics of the Earth and Planetary Interiors* (2008), doi:10.1016/j.pepi.2009.07.012

This is a PDF file of an unedited manuscript that has been accepted for publication. As a service to our customers we are providing this early version of the manuscript. The manuscript will undergo copyediting, typesetting, and review of the resulting proof before it is published in its final form. Please note that during the production process errors may be discovered which could affect the content, and all legal disclaimers that apply to the journal pertain.

Volcanic unrest of the Colli Albani (central Italy)**detected by GPS monitoring test**

F. Riguzzi, G. Pietrantonio, R. Devoti, S. Atzori, M. Anzidei

Istituto Nazionale di Geofisica e Vulcanologia, sez. CNT, Rome, Italy

Abstract

The Colli Albani volcanic complex, located in central Italy about 15 km SE of Rome, has been dominated by periodic eruptive histories started about 561 ka and ending with the most recent and voluminous activity of the Albano maar (<70 ka) phase. Earthquakes of moderate intensity, gas emissions and significant ground deformations are the recent evidences of a residual activity. We decided to start a monitoring test by installing as first step three GPS permanent stations on the volcanic structure, in sites easily accessible. The analysis of about two years of GPS observations has evidenced a peculiar velocity pattern of the Colli Albani stations with respect to those located nearby, but outside the volcano edifice. With respect to Eurasia, the horizontal velocities are NE directed with magnitudes of 2.2 ± 1.4 mm/yr (RDPI), 3.0 ± 0.8 mm/yr (RMPO) and 3.3 ± 1.2 mm/yr (NEMI). The uplift rates are determined with minor accuracy and range from 3.3 and 6.0 mm/yr. We used a nonlinear inversion algorithm to determine the best-fit parameters for a Mogi spherical source based on the Levenberg-Marquardt least-squares approach. The best fit is obtained with a source at 4.6 km depth beneath the western flank of the volcano and a volume variation of $3.6 \cdot 10^{-4}$ km³/yr. This result is in agreement with the volume rate retrieved by PS InSAR technique and rather different from the rate inferred from leveling surveys. Consequently, non-linear trends of the hydrothermal system charge cannot be excluded a priori and the continuous GPS monitoring should be considered a priority in assessing the hazard of the Colli Albani.

25 **Introduction**

26 The Colli Albani volcanic complex is located in central Italy, about 15 km SE of Rome, in an area
27 belonging to the potassic and ultrapotassic Roman Magmatic Province, a northwest-trending chain of
28 volcanoes that developed along the Tyrrhenian Sea margin of Italy during middle and late Pleistocene
29 time (De Rita et al., 1988; Trigila, 1995). The volcanic history of the Colli Albani is dominated by
30 periodic eruptive histories started about 561 ka and ending with the most recent and voluminous
31 activity of the Albano maar (<70 ka) phase, that cannot be considered completely extinguished (Freda
32 et al., 2006; Funicello et al., 2003).

33 Seismic activity and gas emissions are considered the main risk source for the villages located in the
34 Colli Albani area, whereas it is not yet clear which could be the level of hazard due to slow
35 deformations. In fact, this area is characterized by recurrent seismic activity (Feuillet et al., 2004;
36 Tertulliani and Riguzzi, 1995; Chiarabba et al., 1994; Amato et al., 1994 and reference therein);
37 temperature and water composition variations (Boni et al., 1995; Calcara et al., 1995, Carapezza et al.,
38 2008); gas emissions, CO₂ and in minor part H₂S (Carapezza et al., 2008; Carapezza and Tarchini,
39 2007; Tuccimei et al., 2006; Carapezza et al., 2003; Pizzino et al., 2002; Chiodini and Frondini, 2001
40 and reference therein) and by significant ground deformations detected by high precision leveling and
41 PS-InSAR time series. The mean rate of uplift has been estimated from 3 to 7 mm/yr, from PS-InSAR
42 and leveling surveys respectively, on very different time spans (Amato and Chiarabba 1995; Salvi et
43 al., 2004).

44 Seismic swarms originate recurrently in the more recent volcanic structures, the freatomagmatic
45 craters of the West side of the Colli Albani, in particular the Albano crater (Amato et al., 1994). Seismic
46 tomography analyses recognized the presence of a low velocity volume, identified as magmatic
47 chamber, located about 6 km below this recent area; on the contrary, a high velocity volume was
48 identified under the oldest part of the volcano (Chiarabba et al. 1997). The analysis of the teleseismic

49 receiver functions has shown the crustal and uppermost mantle structure beneath the Colli Albani; the
50 Moho is almost flat and located at 23 km, a shallow limestone layer with a variable thickness is present
51 between 4 and 5 km; however, a local complexity of the crustal structure changing from site to site has
52 been also detected (Bianchi et al., 2008).

53 During the last few years, a series of papers on geochronology (Freda et al., 2006; Marra and Karner,
54 2005), stratigraphic and physical properties from down hole drilling (Mariucci et al., 2008),
55 experiments on the magma composition (Freda et al., 2008) and eruption products (Sottili et al., 2008)
56 have shed new light on the history and present physical state of the volcanic structure.

57 Other works (Funicello et al., 2002; Funicello et al., 2003; Anzidei et al., 2008) highlighted the
58 relevance of high water level variations and catastrophic withdrawal of the Albano maar lake since pre-
59 historic age as possible indicators of sudden variation of CO₂ flow and upwelling of hydrothermal
60 fluids (Carapezza et al., 2008).

61 A comprehensive hazard assessment of active and quiescent volcanoes may strongly depend from the
62 morphology of the edifice structure. The landslide hazard evaluation must take into account the
63 presence of sub-aerial and submerged unstable slopes identified in the more recent craters of the Colli
64 Albani (Bozzano et al. 2009), whose detection is necessarily based on the knowledge of a detailed
65 digital terrain model (DTM). Therefore, from 2005 to 2007 three different surveys (high precision
66 bathymetric survey of the Albano lake (Anzidei et al., 2006), airborne laser scanning (ALS) and
67 GNSS/RTK survey have been carried out to obtain a high resolution DTM of the area and an
68 estimation of the water volume variations of the Albano lake (Pietrantonio et al., 2008; Riguzzi et al.,
69 2008).

70 Most of these researches have been supported by the Department of the Civil Protection through the
71 project DPC115 V3_1, specifically oriented to the definition of potential hazards and crisis levels of the
72 Colli Albani. Considering gas emissions, seismic swarms and ground deformation the most compelling

73 unrest activities of the volcano, one of the priority of the project has been to study the dynamics of the
74 area and their interferences with human activities, including local-scale ground deformation, stress
75 field, slope stability, recent eruptive processes, crater lake evolution, quaternary mass flows.

76 In this framework, we decided to start a monitoring test at the Colli Albani area by installing as first
77 step three GPS permanent stations in sites easily accessible. With respect to non-permanent networks
78 (Betti et al., 1999; Anzidei et al., 1998), the continuous monitoring highly improves the accuracy of site
79 velocity estimations by the analysis of long time series of GPS observations (Devoti et al., 2008). The
80 recent development and densification of GPS permanent networks in Italy, in particular the realization
81 of the RING network (<http://ring.gm.ingv.it>, Selvaggi et al., 2006) offers the opportunity to anchor the
82 velocity field of local networks to internationally defined reference systems, currently the ITRF2005
83 (Altamimi et al., 2007), and then to refer local motion in a regional tectonic context.

84 As underlined in Salvi et al. (2004), unlike other Italian volcanoes, the Colli Albani has not undergone
85 extensive monitoring for long time periods; this gap must be rapidly filled to lay the basis for a more
86 complete assessment of volcanic hazard in such a strongly inhabited and vulnerable area.

87

88 **Test sites and GPS data processing**

89 We selected the three test sites in locations easily accessible, with electric power facilities:
90 Monteporzio Catone (RMPO), at the Astronomical Observatory; Rocca di Papa (RDPI) at the INGV
91 Observatory, and Nemi (NEMI), at the Padri Verbiti monastery. RMPO is located on the external belt
92 of the Tuscolano-Artemisio caldera, RDPI on the Faete caldera and NEMI on the border separating the
93 ancient Tuscolano-Artemisio caldera and the recent Nemi maar, where together with the Albano and
94 Ariccia maare, the last hydro-magmatic phase took place (Figure 1).

95 The monument of RMPO is a reinforced concrete column where is immersed a perpendicular steel rod
96 on which the antenna is screwed on. RDPI and NEMI are realized on reinforced concrete buildings

97 with a particular mounting consisting of a short steel pillar (0.65m height) screwed on a steel
98 benchmark permanently and deeply fixed to the top of the building. The antenna is screwed on the top
99 of the pillar and settled in horizontal position through 2 spherical spirit bubbles and 3 screws. Such
100 monument preserves the horizontal and vertical datum when the antenna has to be changed.

101 RMPO and RDPI are equipped with receivers LEICA GRX1200PRO and LEIAT504 choke-ring
102 antennas (RMPO with radome LEIS, see Figure 1), NEMI is equipped with receiver TRIMBLE 5700
103 and Zephyr Geodetic antenna TRM41249.00.

104 We have analyzed the GPS observations at 30 s sampling rates of the Colli Albani test sites in the
105 framework of the processing of all the Italian permanent stations. Consequently, the whole network is
106 divided into 11 clusters of more than 40 stations each one, sharing 11 common anchor sites, i.e.
107 selected sites based on station performance and geographical distribution, subsequently used as core
108 sites for the cluster combination. NEMI, RDPI and RMPO started to work in the middle of 2006, so
109 their data processing covers about 2.5 years.

110 The data analysis is performed by the *Bernese Processing Engine* (BPE) of the software Bernese 5.0
111 (Beutler et al., 2007), using the phase double differences as observables. The IGS precise orbits and
112 Earth's orientation parameters are kept fixed and the absolute elevation-dependent phase centre
113 corrections, provided by IGS, are applied. We have estimated each daily solution in a *loosely*
114 *constrained* reference frame, close to the rank deficiency condition. Each *loosely constrained* solution
115 is realized in an intrinsic reference frame, defined by the observations itself, differing from day to day
116 only for rigid network translations, keeping the site inter-distances always well determined. The
117 constraints for the realization of the chosen reference frame are imposed only *a posteriori*. The daily
118 *loosely constrained* cluster solutions are then merged into global daily *loosely constrained* solutions of
119 the whole network applying a classical least squares approach (Bianco et al., 2003).

120 We have estimated the velocity field by a purposely designed software (NEVE) that manages the
 121 complete stochastic model. The velocity field is estimated by fitting the *loosely constrained* time series
 122 of daily coordinates with the complete covariance matrix, obtaining a *loosely constrained* velocity
 123 solution. We simultaneously estimate site velocities together with annual signals and sporadic offsets at
 124 epochs of instrumental changes, according to the following functional model

$$125 \quad x_i = x_0 + r \cdot t_i + \alpha \cdot \sin(\omega t_i + \varphi) + \Delta x \cdot H_i \equiv A \cdot y$$

126 where x_0 is the constant, r the rate, α and φ are respectively the amplitude and phase of the annual
 127 signal and H is the Heaviside function useful to detect eventual coordinate offsets (Δx) in the time
 128 series.

129 The unknown parameters of the least squares problem are the components of the vector

$$130 \quad y = (x_0, r, \alpha, \varphi, \Delta x)^T$$

131 and its estimation reads

$$132 \quad \hat{y} = (A^T C_x^{-1} A)^{-1} A^T C_x^{-1} x$$

133 where A is the design matrix, x the observation vector and C_x is the covariance matrix of the
 134 observations.

135 The loosely constrained velocity field is then minimally constrained and transformed into the
 136 ITRF2005 reference frame (Altamimi et al., 2007) by a 14 parameter Helmert transformation. The
 137 errors associated to the velocities derive from the direct propagation of the daily covariance matrices
 138 and from the final minimal constraints operator on the loosely constrained velocity field. Concerning
 139 the whole network, the most recent sites (2 years of observations) show an uncertainty of 1.5 mm/yr
 140 and 3.5 mm/yr respectively in the horizontal and vertical components reaching values down to 0.3
 141 mm/yr and 0.9 mm/yr for the long lasting sites. These errors reflect consistently the expected
 142 repeatability of regional velocity field solutions obtained with different methods (e.g. Devoti et al.,
 143 2008; Serpelloni et al., 2005).

144 Figure 2 shows the time series of the N, E, Up coordinates in the ITRF2005 reference frame for the
145 three test sites.

146 A more effective representation of the velocity field estimated with this procedure is to show the
147 residual velocities with respect to stable Eurasia (Table 1, Figure 3), whose kinematics is defined
148 through the rotation pole and rate estimated in Devoti et al. (2008).

149 The Italian area is the region of the interaction between the African and the Eurasian plates, where the
150 lithosphere is deformed and fragmented in minor blocks, the main of these is the Adriatic plate. The
151 Apennines belt is the chain crossing axially the whole Italian peninsula from NW to SE, it is formed as
152 accretionary prism of the Neogene to present arcuate W-directed subduction of the Adriatic plate. The
153 eastward retreat of the subduction is commonly considered as the most plausible explanation for the
154 progressive eastward migration of the thrust fronts (Scrocca, 2006). This retreating is at present well
155 testified by the GPS velocity pattern having the main direction toward NE with respect to the Eurasian
156 reference frame (Devoti et al., 2008). Then, on average, the Apennine belt constitutes the natural
157 separation of the Italian peninsular velocity field, sites located on the western side display NW-directed
158 velocities whereas sites located on the eastern side display NE-directed velocities.

159 The Eurasian fixed representation highlights a different trend between the horizontal velocities of the
160 Colli Albani sites (NE-directed) with respect to those located in Rome (NW-directed), about 20 km
161 apart from them (Figure 3).

162 The three roman sites (INGR, M0SE and ROMA) have a coherent motion with the GPS velocities of
163 sites located along the Tyrrhenian belt, with the above mentioned documented linear trend decreasing
164 from SE to NW (Devoti et al., 2008). The different behavior of the Colli Albani with respect to the
165 Tyrrhenian sites is better evidenced showing their residual velocities with respect to the roman sites
166 (Table 2, Figure 4).

167

168 **GPS data modeling**

169 To model the source of deformations, we have referred the GPS velocities with respect to the roman
170 sites (INGR, M0SE, ROMA) with the aim to remove any regional pattern from the local velocity field.

171 We model GPS data by a Mogi point-pressure source (Mogi, 1958). The underlying reason for the use
172 of such simple model is the low number of available observations (14 measurements from 6 GPS
173 stations, 4 rejected a priori due to clear local effects) that prevents the use of more complex sources like
174 a prolate ellipsoid (Yang et al., 1988) or a sill/dike (Okada, 1985). In fact, though these sources are
175 more realistic and advisable (Salvi et al., 2004; Tizzani et al., 2009), they cannot be used with such a
176 low number of observations, unless constraining most of the parameters, either from external
177 observation or from literature.

178 A Mogi source is defined with only 4 parameters that we can set completely free in the nonlinear
179 inversion. Despite the simplicity of the assumption about the medium (an isotropic and homogeneous
180 half-space with no topography), we can assume that the discrepancy between the Mogi model and a
181 finite element model accounting for the topography falls in the data uncertainty. From Kirchdörfer
182 (1999) is evident that the last assumption is stronger as the source is deeper: in our modeling the source
183 depth is about 5 km in comparison to highest GPS station located at 700 m.

184 Under these remarks, we retrieve the source parameters by a non-linear inversion based on the
185 Levenberg-Marquardt (LM) least-squares approach. The LM algorithm is one of the most efficient and
186 widely used optimization algorithm consisting in a combination of a gradient descent and Gauss-
187 Newton iteration (Levenberg, 1944; Marquardt, 1986). Our implementation of the LM comes from the
188 Fortran MINPACK library (Morè et al., 1980); it is written in IDL and modified with multiple random
189 restarts to guarantee the detection of the global minimum in the optimization process. The cost function
190 is a simple minded weighted mean of the residuals of the form:

191

$$CostFunction = \frac{1}{N} \sum_i^N \frac{(d_{i,obs} - d_{i,mod})^2}{\sigma_i}$$

192

where $d_{i,obs}$ and $d_{i,mod}$ are the observed and modelled displacement of the i -th point and σ_i is the

193

standard deviation.

194

The best-fit parameters are shown in Table 2, together with the relative standard deviations and the

195

range of values allowed in the inversion. The nonlinear inversion sets the point-source at a depth of

196

about 4.7 km, on the western flank of the Colli Albani complex (see Figure 5). Such results are in a

197

good agreement with those from Salvi et al., 2004, where a prolate ellipsoid double source is used to

198

model DInSAR data.

199

The displacement is modulated by ΔK , a free parameter that can be converted in terms of volume or

200

pressure variation through the following equations:

201

$$\Delta K = \frac{\Delta V}{\pi} \qquad \Delta K = \Delta P \cdot \frac{R^3}{\mu}$$

202

where ΔV is the volume variation, ΔP is the pressure variation for a given value of the radius R . In

203

terms of volume, the best-fit solution corresponds to an increase of $1.14 \cdot 10^6 \text{ m}^3/\text{yr}$. This solution yields

204

a cost function of 0.62 (the cost function corresponding to the null solution, i.e. the data themselves, is

205

1.57). The observed and modelled rates are reported in Table 4.

206

A careful analysis of the uncertainty and the trade-offs affecting the source parameters is also provided.

207

This analysis is performed by perturbing every GPS measurement by a noise source whose value is

208

randomly sampled from a Gaussian distribution with standard deviation equal to that of the considered

209

point. In order to derive how the data uncertainty is mapped to the model parameters, we generate

210

hundreds of perturbed dataset rerunning, each time, the nonlinear inversion. This technique is widely

211

used in the assessment of the model parameters uncertainty (Funning et al., 2005; Parsons et al., 2006;

212

Tizzani et al., 2009) allowing the estimate of the parameter standard deviations and possible trade-offs

213

(Figure 6).

214

215 **Discussion and conclusion**

216 We have installed three test sites of continuous GPS monitoring on the Colli Albani volcanic complex
217 to evaluate the velocity components and the achievable accuracies. The sites were selected where
218 power and location facilities made logistically convenient the test. Two observatories and a monastery
219 have satisfied these basic requirements; nevertheless, it has to be underlined this simple network does
220 not assure a suitable azimuthal distribution, since the stations are all located on the eastern flank of the
221 area where the maximum uplift has been detected by PS InSAR technique.

222 After about 2.5 years of continuous monitoring the results are very encouraging and suggest increasing
223 the number of stations to close the azimuth gap toward SW. The time series analysis of coordinates,
224 after the removal of outliers and instrumental/modeling offsets, has allowed estimating velocities with
225 good accuracy .

226 With respect to Eurasia, the horizontal velocities of the Colli Albani sites are NE directed with
227 magnitudes of 2.2 ± 1.4 mm/yr (RDPI), 3.0 ± 0.8 mm/yr (RMPO) and 3.3 ± 1.2 mm/yr (NEMI). As known,
228 GPS vertical rates are determined with minor accuracy with respect to the horizontal; in our case we
229 obtain 4.7 ± 5.2 mm/yr (RDPI), 3.3 ± 3.5 mm/yr (RMPO) and 6.0 ± 5.0 mm/yr (NEMI). The accuracies of
230 the rate estimations depend basically on the length of the observation series: long lasting stations can
231 reach accuracies better than mm/yr level, even in the vertical component as shown for INGR and
232 MOSE (Table 1).

233 The determination of accurate uplift rates on volcanoes is very important, in particular in the Colli
234 Albani area, where vertical motion has been mostly detected till now (Amato and Charabba, 1995;
235 Salvi et al., 2004). Salvi et al. (2004) have shown that present deformation is concentrated in the area of
236 most recent volcanic activity and the inversion of the observed deformation best fits the data if two

237 Mogi sources aligned in a N-S direction at 5 and 7 km depth beneath the western flank of the volcano
238 are considered.

239 From our GPS test, the best-estimated Mogi source (Table 2) is located in the area of the most recent
240 volcanic activity where several phreatomagmatic explosions occurred, generating the Albano, Ariccia
241 and Nemi maare and some coalescent craters. In spite of the poor azimuthal coverage, the estimated
242 parameters (Table 3) are quite in agreement with those of Salvi et al. (2004) and provide indications
243 about the location of future GPS stations.

244 The horizontal GPS and modeled velocities of the sites located on the volcanic edifice are E- NE
245 directed with magnitudes ranging between 2.7 and 3.3 mm/yr (Table 4, Figure 5). Our data confirm the
246 uplift trend evidenced by other techniques (leveling survey and PS-InSar), but if taken singularly, at
247 this time, appear poorly significant. Nevertheless, plotting the uplift rate of each GPS site vs the
248 distance between the site itself and the center of the estimated Mogi source shown in Figure 5, a clear
249 significant decrease is evidenced. The modeled and GPS uplift trends well agree within the errors, even
250 if the predicted rates appear underestimated with respect to those obtained from GPS (Figure 7).

251 Another source of uplift could be the flexural-isostatic response to unloading due to the water
252 withdrawal of the Albano lake. Based on the integrated DTM and the recent estimated water level
253 values, we have evaluated about $21.7 \cdot 10^6 \text{ m}^3$ the water volume loss of the Albano lake from 1993 to
254 2007, with an average rate of about $1.6 \cdot 10^6 \text{ m}^3/\text{yr}$ (Riguzzi et al., 2008). We have evaluated that the
255 total unloading effect could produce in this area uplift within 1 mm (Turcotte and Schubert, 1982), less
256 than 0.1mm/yr, and then it can be considered negligible for our purposes.

257 It has been stressed that both modern seismicity and ground uplifts detected by leveling surveys can be
258 explained by the accumulation of magma of about $94 \cdot 10^6 \text{ m}^3$ during 43 years, approximately 6 km
259 beneath the zone of seismicity (Feuillet et al., 2004). Hypothesizing a linear trend for the magma

260 accumulation, we can infer a volume change rate of about $21.9 \cdot 10^{-4} \text{ km}^3/\text{yr}$, more than five times the
261 values estimated by GPS and PS-InSAR techniques.

262 However, non-linear trends of the hydrothermal system charge variations cannot be excluded a priori;
263 our speculation is based on the fact that during different time spans different volume rates of the Mogi
264 sources have been inferred from different techniques (Table 3), so that the continuous GPS monitoring
265 should be considered a priority in assessing the hazard of this volcano.

266 For the first time, continuous GPS observations have detected deformations of the Colli Albani
267 volcanic structure. The best-fit inversion of GPS velocities is obtained with a Mogi source model,
268 whose parameters are estimated with good accuracy. Our results are in agreement with those retrieved
269 by other techniques, in spite of the poor azimuthal coverage of our sites mainly located on the eastern
270 flank of the area of maximum uplift; at the same time we could expect a velocity W-ward trend of
271 hypothetical GPS sites located on the western flank. Figure 7 shows the circles of equal horizontal
272 velocities at intervals of 0.5 mm/yr. The predicted velocities have a radial pattern from the source
273 reaching the maximum value at about 5 km from the Mogi source where 4.5 mm/yr are expected, thus
274 providing clear indications for future GPS site deployments.

275 Nevertheless, this work represent a first step and after about three years, the aim of this test seems
276 largely fulfilled; the results achieved till now encourage us to establish new GPS permanent stations
277 primarily on the SW flank of Colli Albani volcano, taking into account the predicted pattern.

278

279 **Acknowledgments**

280 This work has been partially supported by the Dept. of Civil Protection, Project DPC115_V3 Colli
281 Albani. We wish to thank Alessandra Esposito, Angelo Massucci and Sergio Del Mese for their
282 technical support and all the persons involved in the permanent GPS network maintenance. Some of the
283 figures were made by GMT (Wessel and Smith, 1995).

284

285 **References**

- 286 Altamimi, Z., X., Collilieux, J., Legrand, B., Garayt, C., Boucher, 2007. ITRF2005: A new release of
287 the International Terrestrial Reference Frame based on time series of station positions and Earth
288 Orientation Parameters. *J. Geophys. Res.*, 112, B09401, doi:10.1029/2007JB004949
- 289 Amato, A., Chiarabba, C., Cocco, M., Di Bona, M. and Selvaggi, G., The 1989-1990 seismic swarm in
290 the Alban Hills volcanic area, central Italy, *J. Volcanol. Geotherm. Res.*, 61, 225-237, 1994.
- 291 Amato, A. and Chiarabba, C., Recent uplift of the Alban Hills volcano (Italy), evidence for magmatic
292 inflation?, *Geophys. Res. Lett.*, 22, 1985-1988, 1995.
- 293 Anzidei, M., Baldi, P., Casula, G., Galvani, A., Riguzzi, F. and Zanutta, A., Evidence of active crustal
294 deformation of the Colli Albani volcanic area (central Italy) by GPS surveys, *J. Volcanol.*
295 *Geotherm. Res.*, 80, 55-65, 1998.
- 296 Anzidei, M., Esposito, A. and De Giosa, F., The dark side of the Albano crater lake, *Annals of*
297 *Geophysics*, 49, 6, 1275-1287, 2006.
- 298 Anzidei, M., Carapezza, M. L., Esposito, A., Giordano, G., Lelli, M. and Tarchini, L., The Albano
299 Maar Lake high resolution bathymetry and dissolved CO₂ budget (Colli Albani volcano, Italy):
300 constrains to hazard evaluation, *J. Volcanol. Geotherm. Res.*, 171, 3/4, 258-268, 2008.
- 301 Betti, B., Biagi, L., Crespi, M. and Riguzzi, F., GPS sensitivity analysis applied to non-permanent
302 deformation control networks, *J. Geodesy*, 73, 3, 158-167, 1999.
- 303 Beutler et al., 2007, Bernese GPS Software. In: Dach R., Hugentobler U., Fridez P., Meindl M. (Eds),
304 *Astronomical Institute, University of Bern (January 2007).*
- 305 Bianchi, I., Piana Agostinetti, N., De Gori, P. and Chiarabba, C., Deep structure of the Colli Albani
306 volcanic district (central Italy) from receiver functions analysis, *J. Geophys. Res.*, 113, B09313, ,
307 doi:10.1029/2007JB005548, 2008.

- 308 Bianco, G., Devoti, R., Luceri, V., 2003. Combination of loosely constrained solutions. IERS Tech.
309 Note (30), 107–109.
- 310 Boni, C., Bono, P., Lombardi, S., Mastroiillo, L. and Percopo, C., Hydrogeology, fluid chemistry, and
311 thermalism, in The volcano of the Alban Hills, edited by Raffaello Trigila, University of Rome *La*
312 *Sapienza*, Roma, 221-240, 1995.
- 313 Bozzano, F., Mazzanti, P., Anzidei, M., Esposito, C., Floris, M., Bianchi Fasani, G., and Esposito, A.,
314 Slope dynamics of Lake Albano (Rome, Italy): insights from high resolution bathymetry, *Earth Surf.*
315 *Process. Landforms*, in press, 2009.
- 316 Calcara, M., Lombardi, S. and Quattrocchi, F., Geochemical monitoring for seismic surveillance, in
317 The volcano of the Alban Hills, edited by Raffaello Trigila, University of Rome *La Sapienza*, Roma,
318 243-263, 1995.
- 319 Carapezza, M.L., Badalamenti, B., Cavarra, L. and Scalzo, A., Gas hazard assessment in a densely
320 inhabited area of Colli Albani Volcano (Cava dei Selci, Roma), *J. Volcanol. Geotherm. Res.* 123,
321 81–94, 2003.
- 322 Carapezza, M.L. and Tarchini, L., Accidental gas emission from shallow pressurized aquifers at Alban
323 Hills volcano (Rome, Italy): Geochemical evidence of magmatic degassing?, *J. Volcanol.*
324 *Geotherm. Res.*, 165, 5-16, 2007.
- 325 Carapezza. M.L., Lelli, M. and Tarchini, L., Geochemistry of the Albano and Nemi crater lakes in the
326 volcanic district of Alban Hills (Rome, Italy), *J. Volcan. Geoth. Res.*, 178, 2, 297-304, 2008.
- 327 Cavaliè, O., Doin, M.-P., Lasserre, C. and Briole, P., Ground motion measurement in the Lake Mead
328 area, Nevada, by differential synthetic aperture radar interferometry time series analysis: Probing the
329 lithosphere rheological structure, *J. Geophys. Res.*, 112, B03403, doi:10.1029/2006JB004344, 2007.
- 330 Chiarabba, C., L. Malagnini, and A. Amato, Three-dimensional velocity structure and earthquakes
331 relocation in the Alban Hills volcano, central Italy, *Bull. Seismol. Soc. Am.*, 84(2), 295–306, 1994.

- 332 Chiarabba, C., Amato, A. and Delaney, P.T., Crustal structure, evolution and volcanic unrest of the
333 Alban Hills, Central Italy, *Bull. Volcanol.*, 59, 161-170, 1997.
- 334 Chiodini, G. and Frondini, F., Carbon dioxide degassing from the Albani Hills volcanic region, Central
335 Italy, *Chem. Geol.*, 177, 67-83, 2001.
- 336 De Rita, D., Funiciello, R. and Parotto, M., Geological Map of the Alban Hills Volcanic Complex,
337 CNR, Rome, 1988.
- 338 Devoti, R., Riguzzi, F., Cuffaro, M. and Doglioni, C., New GPS constraints on the kinematics of the
339 Apennine subduction, *Earth Planet. Sci. Lett.*, 273, 1-2, 163-174, 2008.
- 340 Feuillet, N., Nostro, C., Chiarabba, C. and Cocco, M., Coupling between earthquake swarms and
341 volcanic unrest at the Alban Hills Volcano (central Italy) modeled through elastic stress transfer, *J.*
342 *Geophys. Res.*, 109, B02308, doi:10.1029/2003JB002419, 2004.
- 343 Freda, C., Gaeta, M., Karner, D.B., Marra, F., Renne, P.R., Taddeucci, J., Scarlato, P., Christensen,
344 J.N. and Dallai, L., Eruptive history and petrologic evolution of the Albano multiple maar (Alban
345 Hills, Central Italy), *Bull. Volc*, 68, 567-591, DOI 10.1007/s00445-005-0033-6, 2006.
- 346 Freda, C., Gaeta, M., Misiti, V., Mollo, S., Dolfi, D. and Scarlato, P., Magma-carbonate interaction: an
347 experimental study on ultrapotassic rocks from Alban Hills (Central Italy), *Lithos*, 101, 3-4, 397-
348 415, 2008.
- 349 Funiciello, R., Giordano, G. and De Rita, D., The Albano maar lake (Colli Albani Volcano, Italy):
350 recent volcanic activity and evidence of pre-Roman Age catastrophic lahar events, *J. Volcanol.*
351 *Geotherm. Res.*, 123, 1, 43-61, 2003.
- 352 Funning, G. J., B. Parsons, T. J. Wright, J. A. Jackson, and E. J. Fielding, Surface displacements and
353 source parameters of the 2003 Bam, Iran earthquake from Envisat Advanced Synthetic Aperture
354 Radar imagery, *J. Geophys. Res.*, 110(B9), B09406, doi:10.1029/2004JB003338, 2005.

- 355 Kirchdörfer, M., Analysis and quasi-static FE modeling of long period impulsive events associated
356 with explosions at Stromboli volcano (Italy), *Annali di Geofisica*, 42(3), 379-390, 1999.
- 357 Levenberg, K., A Method for the Solution of Certain Non-Linear Problems in Least Squares, *The*
358 *Quarterly of Applied Mathematics*, 2, 164–168, 1944.
- 359 Marquardt, D. , An Algorithm for Least-Squares Estimation of Nonlinear Parameters, *SIAM, J. of*
360 *Applied Mathematics*, 11, 431–441, 1963.
- 361 Marra, F., Karner, D.B., 2005. The Albano maar (Alban Hills volcanic district, Italy): active or dormant
362 volcano? *Il Quaternario* 18-2, 173–185.
- 363 Mariucci, M. T., Pierdominici, S., Pizzino, L., Marra, F., Montone, P., Looking into a volcanic area: An
364 overview on the 350m scientific drilling at Colli Albani (Rome, Italy), *J. Volcanol. Geotherm. Res.*,
365 176, 2, 225-240, 2008.
- 366 Mogi, K. (1958), Relations between eruptions of various volcanoes and the deformation of the ground
367 surface around them, *Bull. Earthquake Res. Inst. Univ. Tokyo*, 36, 99– 134.
- 368 Moré, J.J, Garbow, B.S., and Hillstom, K. E., 1980, User Guide for MINPACK-1: Argonne National
369 Laboratory Report ANL-80–74, 49 p.
- 370 Parsons, B., Wright, T., Rowe, P., Andrews, J., Jackson, J., Walker, R., Khatib, M., Talebian, M.,
371 Bergman, E., and Engdahl, E.R., The 1994 Sefi Dabeh (eastern Iran) earthquakes revisited: New
372 evidence from satellite radar interferometry and carbonate dating about the growth of an active
373 fold above a blind thrust fault: *Geophys. J. Int.*, 164, 202–217, doi: 10.1111/j.1365–
374 246X.2005.02655.x., 2006
- 375 Pietrantonio G., Baiocchi V., Fabiani U., Mazzoni A., Riguzzi F., Morphological updating on the basis
376 of integrated DTMs: study on the Albano and Nemi craters, *Journal of Applied Geodesy*, 2:4, Dec
377 2008.

- 378 Pizzino, L., Galli, G., Mancini, C., Quattrocchi, F. and Scarlato, P, Natural gas hazard (CO_2 , ^{222}Rn)
379 within a quiescent volcanic region and its relations with tectonic; the case of the Ciampino-Marino
380 area, Alban Hills Volcano, Italy, *Natural Hazards*, 27, 3, 257-287, 2002.
- 381 Riguzzi F., Baiocchi V., Mazzoni A., Pietrantonio G., Water level and volume estimations of the
382 Albano and Nemi lakes (central Italy), *Annals of Geophysics*, 51, 4, 2008.
- 383 Salvi, S., Attori, S., Tolomei, C., Allievi, J., Ferretti, A., Rocca, F., Prati, C., Stramondo, S. and
384 Feuillet, N., Inflation rate of the Colli Albani volcanic complex retrieved by the permanent scatterers
385 SAR interferometry technique, *Geophys. Res. Lett.*, 31, 12, 2004.
- 386 Scrocca, D., Thrust front segmentation induced by differential slab retreat in the Apennines (Italy),
387 *Terra Nova*, 18, 154–161, 2006.
- 388 Selvaggi, G., RING working group, La Rete Integrata Nazionale GPS (RING)
389 dell'INGV: una infrastruttura aperta per la ricerca scientifica, X Conferenza
390 Nazionale dell'ASITA, Bolzano (Italy) 14–17 November, 2006.
- 391 Serpelloni, E., Anzidei, M., Baldi, P., Casula, G., Galvani, A., Pesci, A. and Riguzzi, F., Geodetic
392 deformations in the Central-Southern Apennines (Italy) from repeated GPS surveys, *Annali di*
393 *Geofisica*, 44, 3, 627-647, 2001.
- 394 Serpelloni, E., Anzidei, M., Baldi, P., Casula, G., Galvani, Crustal velocity and strain-rate fields in
395 Italy and surrounding regions: new results from the analysis of permanent and non-permanent GPS
396 network, *Geophys. J. Int.*, 161, 861-880, 2005.
- 397 Sottili. G., Taddeucci, J., Palladino, D.M., Gaeta, M., Scarlato, P. and Ventura, G., Sub-surface
398 dynamics and eruptive styles of maars in the Colli Albani Volcanic district, Central Italy, *J.*
399 *Volcanol. Geotherm. Res.*, inpress,
- 400 Tertulliani, A. and Riguzzi, F., Earthquakes in Rome during the past one hundred years, *Ann.*
401 *Geophys.*, 38, 5-6, 581-590, 1995.

- 402 Tizzani, P., Battaglia, M., Zeni, G., Atzori, S., Berardino, P and R. Lanari, (2009) Uplift and magma
403 intrusion at Long Valley caldera from InSAR and gravity measurements, *Geology*, 37, 1; 63–66;
404 doi: 10.1130/G25318A.1
- 405 Trigila, R. (Editor), *The volcano of the Alban Hills*, Tipografia SGS, Rome, 1995.
- 406 Tuccimei, P., Giordano, G. and Tedeschi, M., CO₂ release variations during the last 2000 years at the
407 Colli Albani volcano (Roma, Italy) from speleothems studies, *Earth Planet. Sci. Lett.*, 243, 449-462,
408 2006.
- 409 Turcotte, D.L., and Schubert, G., 1982. *Geodynamics*, Wiley, New York.
- 410 Wessel, P., Smith, W. H. F., 1995. *The Generic Mapping Tools (GMT) version 3.0*. Technical
411 Reference & Cookbook, SOEST/NOAA.
- 412 Yang, X., Davis, P.M., and Dieterich, J.H., Deformation from inflation of a dipping finite prolate
413 spheroid in an elastic half-space as a model for volcanic stressing, *J. Geophys. Res.*, 93, 4249–4257,
414 doi: 10.1029/JB093iB05p04249, 1988.

415 **Figure captions**

416 Figure 1: The Colli Albani volcanic complex and the three test sites.

417 Figure 2: Time series of the North, East and Up components of NEMI, RDPI and RMPO
418 in the ITRF2005 reference frame.

419 Figure 3: Residual velocity field in central Italy with respect to the Eurasian reference
420 frame defined in Devoti et al. (2008). The velocities of the three test sites of the Colli
421 Albani display an azimuth significantly different from the three roman sites of INGR,
422 MOSE and ROMA.

423 Figure 4. Uncertainty (red bars) and trade-offs (scatter plots) of the source parameters. It
424 is evident the presence of a marked correlation between the depth and the K
425 variation, proportional to the change in volume.

426 Figure 5: Residual GPS velocities (black) with respect to the three roman sites (INGR,
427 MOSE and ROMA), location of the Mogi source and modeled velocities (red).

428 Figure 6: Uncertainty (red bars) and trade-offs (scatter plots) of the source parameters. It
429 is evident the presence of a marked correlation between the depth and the K
430 variation, proportional to the change in volume.

431 Figure 7: Observed (red triangles) and predicted (blue open triangles) vertical velocities
432 vs distance of each site from the center of the Mogi source (Table 3). A linear
433 decrease of rates is shown with increasing distances.

434 Figure 8: Circles of predicted equal horizontal velocities at 0.5 mm/yr intervals, their
435 pattern provide indications for future GPS sites

436

437

438

Table 1: Residual velocity components, semi-major and semi-minor axes of error ellipses, azimuth of the semi-major axis with respect to Eurasia, at 68% confidence level

SITE	Lon ° E	Lat ° N	V_E mm/yr	$\pm V_E$ mm/yr	V_N mm/yr	$\pm V_N$ mm/yr	Up mm/yr	$\pm Up$ mm/yr	Smax mm	Smin mm	Azim °
AQUI	13.35	42.37	0.62	0.04	2.34	0.05	0.79	0.12	0.05	0.04	179
AQUN	13.38	42.34	0.09	1.33	1.91	1.10	3.71	3.11	1.33	1.09	98
CERT	12.98	41.95	1.63	1.42	2.19	0.88	3.79	1.68	1.42	0.88	92
CSGP	13.59	42.86	0.94	1.39	2.86	1.58	4.41	4.95	1.59	1.38	-14
FROS	13.35	41.65	0.22	0.97	1.93	1.29	0.97	3.62	1.29	0.97	177
GUAR	13.31	41.79	1.73	1.46	0.86	1.25	0.59	3.46	1.47	1.24	102
INGP	13.32	42.38	1.20	1.12	3.52	1.10	4.94	3.34	1.13	1.09	122
INGR	12.52	41.83	-1.07	0.60	1.20	0.43	1.39	1.07	0.60	0.43	90
ITRA	14.00	42.66	0.94	0.54	2.99	0.62	2.52	2.39	0.63	0.54	-3
LNSS	13.04	42.60	-0.06	0.75	1.65	0.68	-2.85	2.54	0.75	0.68	92
MOSE	12.49	41.89	-1.06	0.57	1.65	0.45	-0.21	1.33	0.57	0.44	93
NEMI	12.72	41.72	2.09	1.23	2.60	1.13	6.12	5.04	1.23	1.13	-96
RDPI	12.71	41.76	1.69	1.49	1.37	1.33	4.73	5.19	1.50	1.31	106
REFO	12.70	42.96	0.14	0.85	1.76	0.43	4.25	2.88	0.85	0.43	91
RENO	13.09	42.79	1.00	0.82	2.34	0.95	3.49	3.84	0.95	0.82	180
REPI	12.00	42.95	-0.03	0.64	1.98	0.59	4.21	2.13	0.64	0.59	94
RETO	12.41	42.78	-0.56	0.79	1.34	0.59	5.94	3.07	0.79	0.59	90
RIET	12.86	42.41	-0.29	0.67	1.32	0.79	-0.03	2.44	0.79	0.67	177
RMPO	12.70	41.81	1.12	0.58	2.79	0.81	3.28	3.46	0.81	0.58	180
ROMA	12.42	41.91	-0.71	0.86	0.89	1.01	-2.12	3.84	1.01	0.86	174
RSTO	14.00	42.66	1.24	0.39	2.24	0.34	0.60	0.66	0.39	0.34	91
TOLF	12.00	42.06	-2.12	0.79	1.84	0.62	1.12	1.47	0.79	0.62	92
UNOV	12.11	42.72	-0.28	0.49	1.04	0.44	5.47	2.33	0.49	0.44	94
UNTR	12.67	42.56	-0.03	0.85	1.29	1.52	1.86	1.81	1.52	0.85	180
VITE	12.12	42.42	-0.43	2.70	1.67	0.66	2.99	3.20	2.70	0.66	90
VVLO	13.62	41.87	-0.38	0.29	1.79	0.32	5.44	0.81	0.32	0.29	180

439

440

441

442

Table 2: Results of the non-linear inversion for the Mogi source. The standard deviation is calculated from the uncertainty affecting the parameters as shown in Figure 4 (red bars). The ΔK parameter can expressed in terms either of volume or pressure variation (see the text).

Parameters	ΔK (m^3/yr)	Depth (km)	East ^a (km)	North ^a (km)
Variation range	$[5 \cdot 10^2, 3 \cdot 10^6]$	[0.00,10.00]	[300.00,310.00]	[4610.00, 4630.00]
Best fit value	$3.64 \cdot 10^5$	4.70	303.35	4620.17
Standard deviation	$6 \cdot 10^4$	0.60	0.53	0.70

443

^a Coordinates are in UTM-WGS84, Zone 33

444

Model	observation time span (yr)	Lon (°E)	Lat (°N)	Depth (km)	ΔV (km ³ /yr)	RMS
PS-InSAR M2 North (Salvi et al., 2004)	8	12.665	41.751	4.6	$2.0 \cdot 10^{-4}$	0.57
PS-InSAR M2 South (Salvi et al., 2004)	8	12.654	41.666	7.2	$4.4 \cdot 10^{-4}$	0.57
levelling S1 (Feuillet et al., 2004)	43	12.687	41.745	4.9	$21.9 \cdot 10^{-4}$	2.00
GPS this paper	2	12.635	41.709	4.6	$3.6 \cdot 10^{-4}$	0.12

445

446

447

448

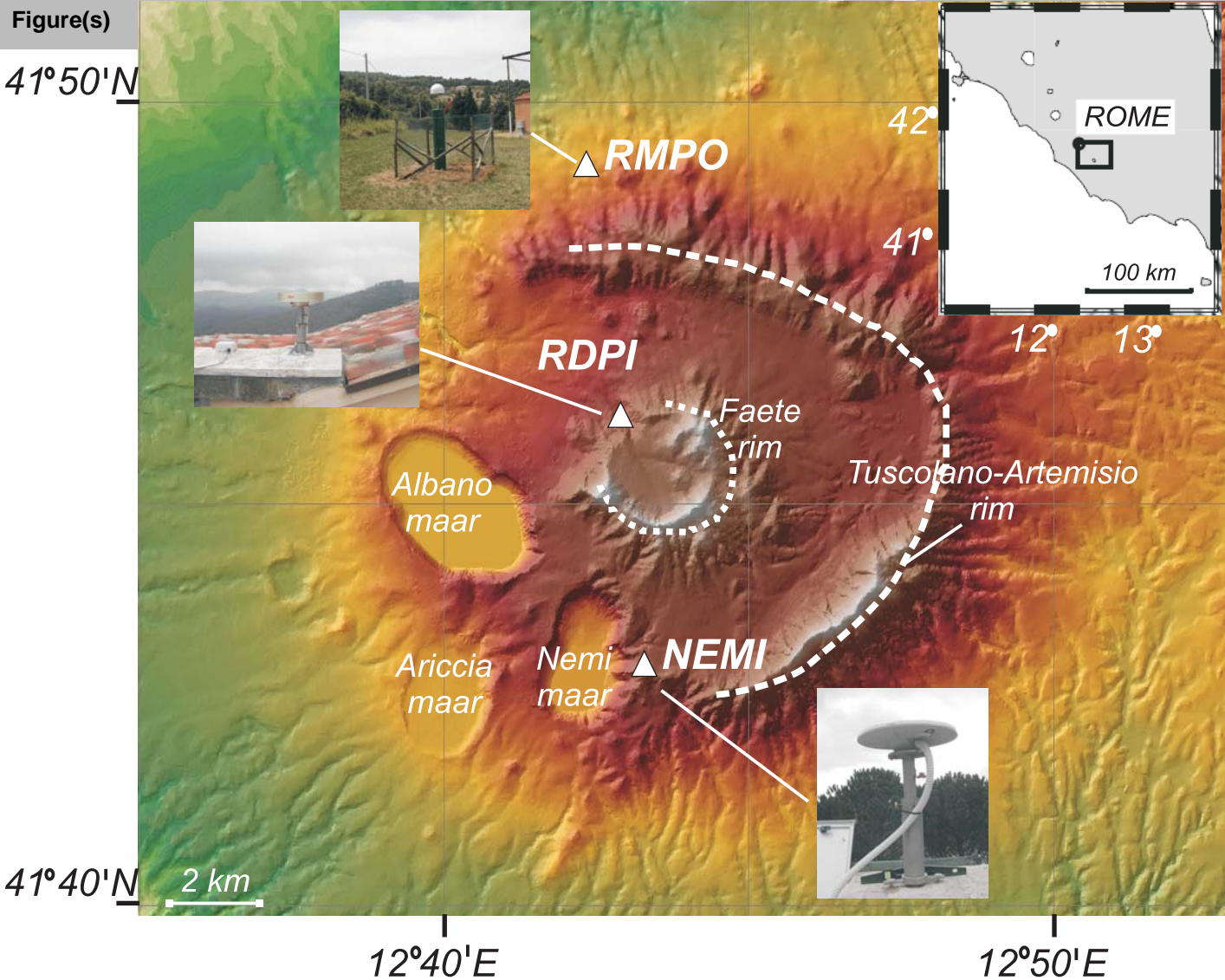
Site	GPS rate components and errors						modeled rates		
	V_E	V_N	Up	$\pm V_E$	$\pm V_N$	$\pm Up$	V_E	V_N	Up
	mm/yr	mm/yr	mm/yr	mm/yr	mm/yr	mm/yr	mm/yr	mm/yr	mm/yr
INGR	0.0	0.0	0.0	0.8	0.6	1.5	-0.51	0.72	0.24
MOSE	0.0	0.4	-1.6	0.8	0.6	1.7	-0.22	-	-
ROMA	0.3	-0.3	-3.5	1.0	1.1	4.0	-0.20	-	-
NEMI	3.2	1.4	4.7	1.4	1.2	5.0	3.26	0.37	2.17
RDPI	2.7	0.2	3.3	1.5	1.3	5.2	1.94	1.69	1.39
RMPO	2.2	1.5	1.9	0.6	0.8	3.5	0.66	1.24	0.51

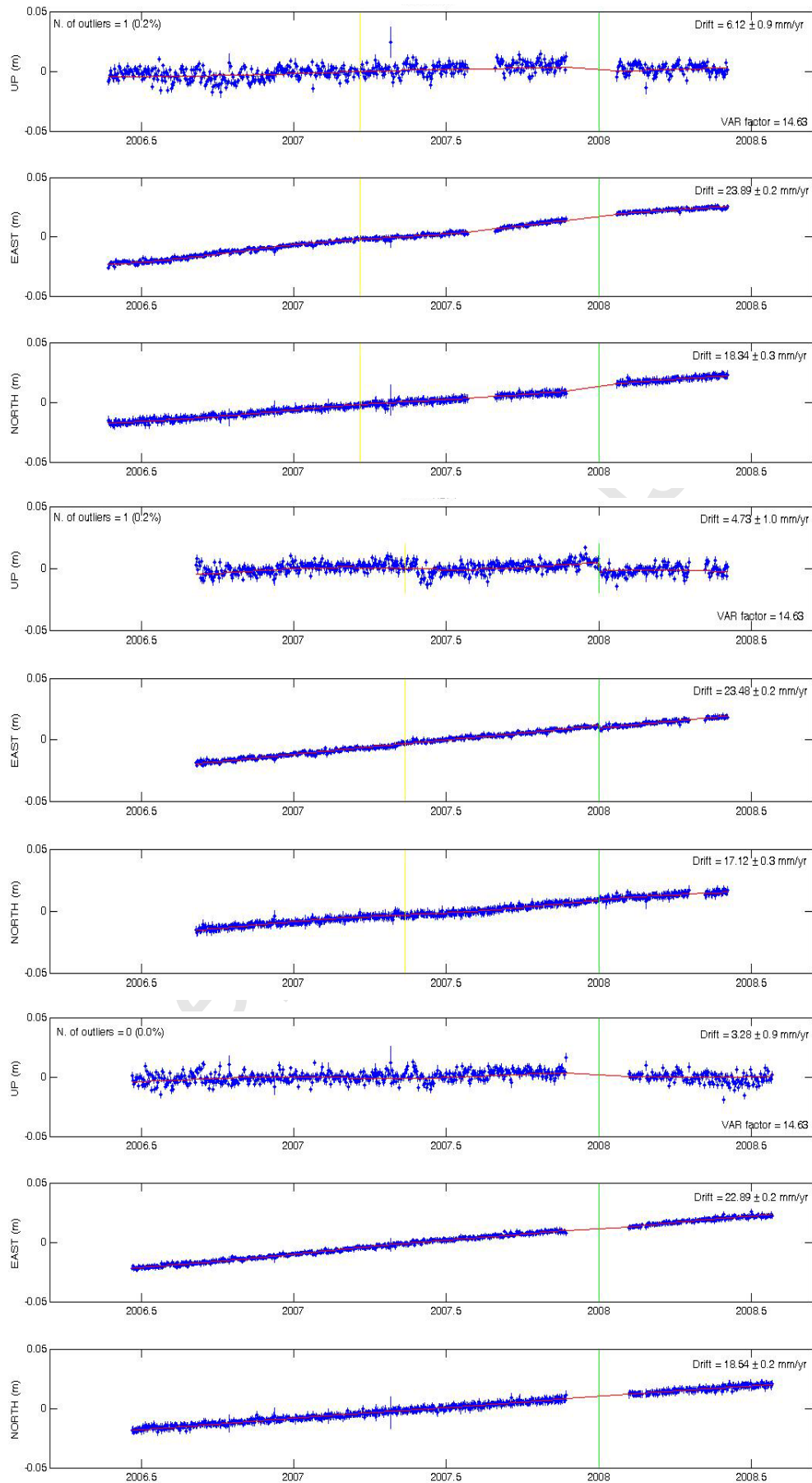
449

450

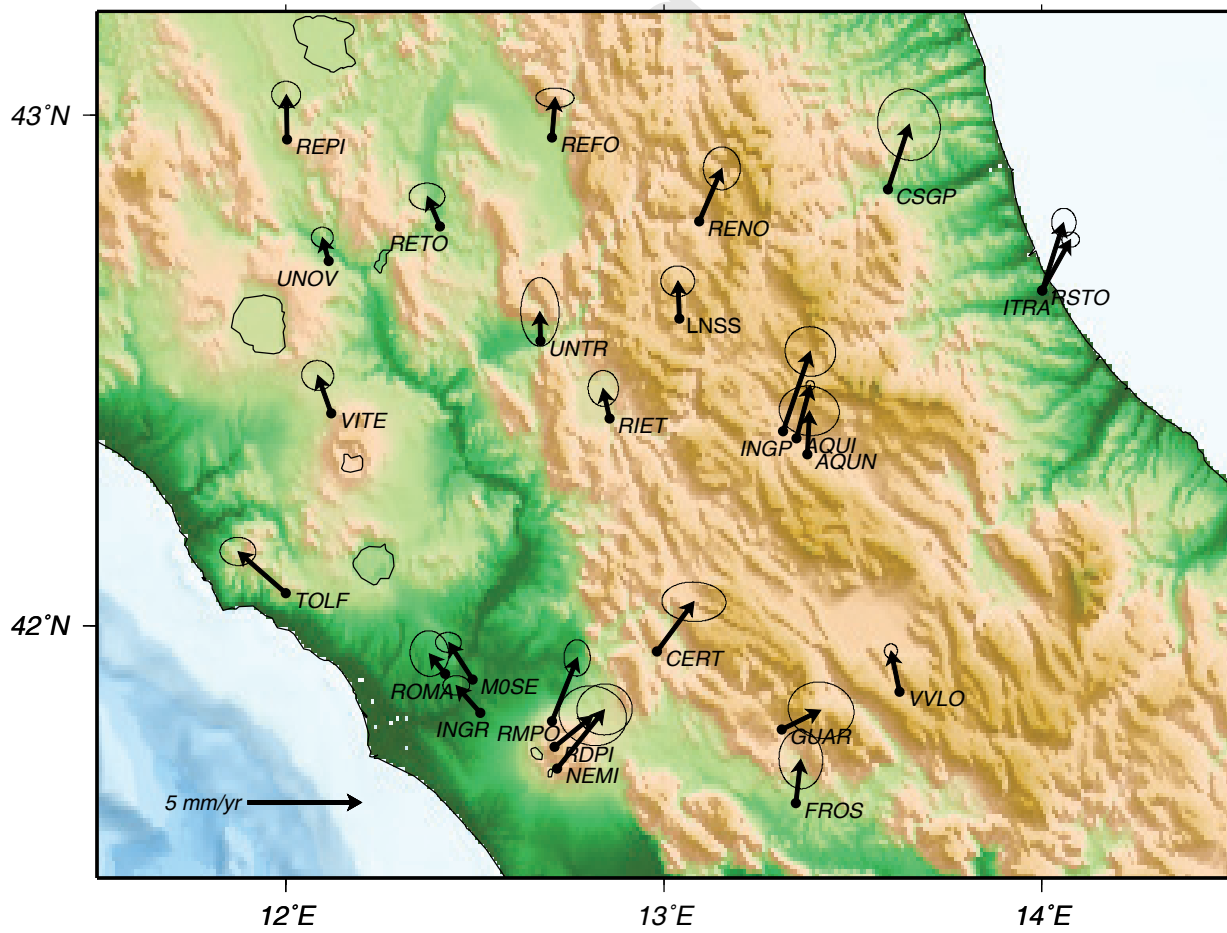
451

452





Manuscript



Manuscript

